2018

Comparison of GMAW and SAW for NGW of 50 mm Q&T Steel Plate

Druce Patrick Dunne
University of Wollongong, druce@uow.edu.au

Willy Pang
Bisalloy Steels

Comparison of GMAW and SAW for NGW of 50 mm Q&T Steel Plate

Abstract

A one-pass-per-layer technique was used for narrow gap welding (NGW) of 50 mm thick plate of quenched and tempered steel with 690 MPa minimum yield strength. GMAW and SAW were investigated for pulsed and non-pulsed welding using the same 1.2 mm strength-matching welding consumable and the same nominal heat inputs for each of the pulsed and non-pulsed welds. The welds were defect-free and the hardness, tensile strength and Charpy impact energies were generally consistent with high weldment integrity. Pulsing of the welding current had the effect of slightly increasing side-wall fusion, flattening the weld bead and decreasing its volume. The most significant differences between the welds produced by GMAW and SAW were that SAW resulted in a lower peak HAZ hardness and higher HAZ Charpy values. These differences arise because different thermal cycles are associated with the two welding processes. Although the nominal heat inputs were the same, the effective heat inputs differed because of the different shielding methods and weld bead profiles. The HAZ hardness and CVN values are consistent with lower cooling rates for the SAW welds.

Keywords

ngw, 50, mm, q&t, saw, steel, comparison, plate, gmaw

Disciplines

Engineering | Science and Technology Studies

Publication Details

Dunne, D. P. & Pang, W. (2018). Comparison of GMAW and SAW for NGW of 50 mm Q&T Steel Plate. Journal of Welding and Joining, 36 (1), 41-49.

ISSN 2466-2232
Online ISSN 2466-2100

Comparison of GMAW and SAW for NGW of 50 mm Q&T Steel Plate

Druce Patrick Dunne*,†, and Willy Pang**

*Faculty of Engineering and Information Sciences, University of Wollongong, NSW, 2522, Australia
**Bisalloy Steels, Unanderra, NSW, 2526, Australia

†Corresponding author : druce@uow.edu.au

(Received March 25, 2017 ; Revised June 2, 2017 ; Accepted November 7, 2017)

Abstract

A one-pass-per-layer technique was used for narrow gap welding (NGW) of 50 mm thick plate of quenched and tempered steel with 690 MPa minimum yield strength. GMAW and SAW were investigated for pulsed and non-pulsed welding using the same 1.2 mm strength-matching welding consumable and the same nominal heat inputs for each of the pulsed and non-pulsed welds. The welds were defect-free and the hardness, tensile strength and Charpy impact energies were generally consistent with high weldment integrity. Pulsing of the welding current had the effect of slightly increasing side-wall fusion, flattening the weld bead and decreasing its volume. The most significant differences between the welds produced by GMAW and SAW were that SAW resulted in a lower peak HAZ hardness and higher HAZ Charpy values. These differences arise because different thermal cycles are associated with the two welding processes. Although the nominal heat inputs were the same, the effective heat inputs differed because of the different shielding methods and weld bead profiles. The HAZ hardness and CVN values are consistent with lower cooling rates for the SAW welds.

Key Words : Narrow gap welding, GMAW, SAW, 50 mm Q&T plate, Mechanical properties

1. Introduction

The term narrow gap welding (NGW) first appeared in an article published in 1966[1], but the procedure was not formally defined until 1981 when it was described by Commission XII of the IIW as an "arc welding process of a narrow-groove joint whose gap is considerably smaller compared with the thickness of the plate to be welded"[2]. However, this definition does not include the most typical and important features of NGW and does not clearly differentiate it from other welding processes that involve a reduced gap.

A more rigorous definition by Malin[3] is "a property-oriented bead-deposition technique associated with an arc welding process and characterized by a constant number of beads per layer that are deposited one on top of the other in a deep, narrow square groove". The distinguishing features of NGW are that: (1) it is produced by arc welding; (2) it is a special bead deposition technique, not a welding process; (3) it features a fixed bead deposition layout; (4) it requires a square groove or one with a small groove angle; and (5) it is a property-oriented technique that necessitates low or medium heat input[4]. Following more recent developments of laser, laser-hot wire and laser-arc hybrid methods for NGW[5-8], point (1) needs to be qualified. However, the other characteristics remain as defining features of NGW.

For arc welded NG joints, small diameter electrodes are generally used to control the heat input. Multi-pass welding results in retempering of weld beads by subsequent overlaying passes in the deep and narrow groove. A narrow heat affected zone (HAZ) is produced with a fine grained weld metal and the microstructures of both regions are relatively homogeneous[9]. The small weld volume and the weld configuration also reduce residual stresses[9]. As well as weld quality, other major advantages of NGW are its cost effectiveness and high productivity for welding of thick plate, particularly of higher strength steels.

Bead deposition layouts are typically one or two passes per layer. For a single straight wire and one pass per layer, lack of side-wall fusion can be an issue. Although this problem can be addressed by employing more complex techniques involving tandem arcs, or oscillating, swinging and rotating arcs[10], lack of side-wall fusion for-one-pass-per-layer welding can be countered by using a relatively high heat input, a wide arc and arc pulsation. NGW is commonly based on the four main arc welding processes: gas metal arc welding, gas tungsten arc welding, submerged arc welding and flux cored arc welding.

GMA-NGW offers ease of arc visual observation, high weld quality, high productivity and cost effectiveness [11]. However, problems can arise due to spattering and magnetic arc blow. SA-NGW has increased in attractiveness over time with improvements in the design of filler metals and fluxes. Although it offers advantages of a high deposition rate and the absence of spattering and arc blow[11], complete slag detachment between passes is necessary to prevent slag entrapment, adding to the weld completion time and increasing the process cost.

This paper compares the microstructures and properties of welds produced in 50 mm plate of Q&T steel using GMA-NGW and SA-NGW, with pulsed and non-pulsed welding currents.

2. Experimental materials and methods

A one-pass per layer technique was used for narrow gap welding of 50 mm thick plate of quenched and tempered (Q&T) steel with 690 MPa min. yield strength[11]. The composition of the Q&T steel is given in Table 1. The steel plate was water quenched from 900℃ and tempered at 600℃, producing the following mechanical properties: 730 MPa yield stress, 805 MPa tensile strength, 70% reduction in area, 26% elongation on 50 mm gauge length, an average hardness 298 HV10, and an average Charpy (CVN) value of 40 J at -20℃.

The base steel has a carbon equivalent value, CE (IIW), of 0.58 and therefore preheat would be recommended to prevent hydrogen cracking after welding.

Narrow gap welding by GMAW and SAW was investigated using pulsed and non-pulsed welding currents and the same 1.2 mm strength-matching welding consumable (L-TEC 120). The welding electrode was a boron-free, low carbon, high Ni steel with significant concentrations of Mn, Si, Cr and Mo. The composition is given in Table 2.

The gap was 10 mm wide at the base and 12 mm wide at the top, producing a 3° gap taper. A 10 mm thick backing plate was used. The constant welding parameters were 200 mm/min. welding speed, 300 A welding current, 120℃ preheat and 150℃ maximum interpass temperature; and the variable welding parameters are recorded in Table 3. For non-pulsed welds the voltage was 30 V and the nominal heat input was 2.70 kJ/mm. The voltage was higher for the pulsed welds (32 V) and the heat input was 2.88 kJ/mm. Argoshield 52 (77% Ar, 23% CO_2) was used for GMAW and 880M flux was used for SAW.

The narrow gap welding equipment was developed by CSIRO in their Adelaide welding laboratory[10,11]. A

Table 3 Welding conditions for Pulsed (P) and Non-Pulsed (NP) narrow gap welding of 50 mm Q&T plate. Constant welding parameters were: current, 300 A; welding speed, 200 mm/min.; electrode, 1.2 mm dia. L-TEC 120; preheat, 120℃; and maximum interpass temperature, 150℃

Welding Method	Gas/Flux	Voltage (V)	Nominal Heat Input (kJ/mm)	Number of passes
P-GMAW	Argoshield 52	32	2.88	9
NP-GMAW	Argoshield 52	30	2.70	9
P-SAW	880M	32	2.88	10
NP-SAW	880M	30	2.70	9

Table 1 Composition (wt%) of 50 mm thick Q&T steel plate used for NGW

%C	%Mn	%P	%Si	%S	%Ni	%Cr	%Mo	%Cu	%Al	%Ti	%B
0.17	1.18	0.016	0.41	0.002	0.025	0.86	0.20	0.015	0.028	0.02	0.0018
0.17	1.18	0.016	0.41	0.002	0.025	0.86	0.20	0.015	0.028	0.02	0.0018

Table 2 Composition (wt%) of weld metal consumable (L-TEC 120) used for NGW

%C	%Mn	%P	%Si	%S	%Ni	%Cr	%Mo	%Cu	%Al	%Ti
0.078	1.63	0.014	0.42	0.007	2.35	0.40	0.55	0.04	0.045	0.02
%B	%O	%N								
<0.0005	0.004	0.0049								

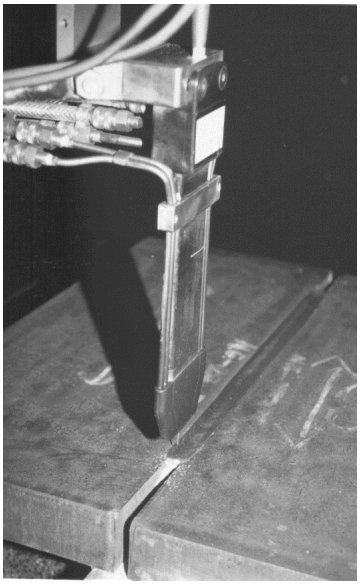

Fig. 1 Photograph of the narrow gap welding equipment used to butt weld the 50 mm Q&T steel plate

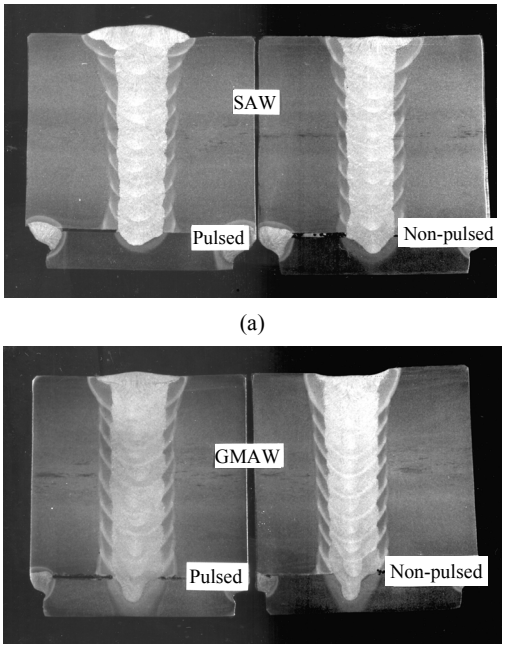

Fig. 2 Macrographs of NG welds in 50 mm Q&T steel plate: NG-SAW (a) and NG-GMAW (b)

one-pass-per-layer technique was used with finer electrodes (1.2 mm) than is typical for many other NGW designs[11]. The welding head was 8 mm wide to enable welding into the 10-12 mm gap. Fig. 1 shows a photograph of the equipment used.

Weld samples were sectioned and metallographically prepared for macroscopic and microscopic examination. Vickers hardness testing was conducted on polished and lightly etched samples, according to the Australian Standard AS2205.6.1[12], to locate indentations relative to the HAZ and fusion boundaries. Charpy impact testing was carried out at -20℃ using cross-weld samples machined from a slab of material (~ 150 mm x 50 mm x 12 mm) cut from a position 3 mm below the top surface. Four Charpy samples were machined from the slab for each of the four welds and light etching was used to locate the V-notch in either the HAZ or the weld metal. The tests conformed to the conditions specified in Australian Standards AS 1544.2[13] and AS 2205.7.1[14]. Cross-weld tensile test samples of 10 mm diameter were machined from the top, middle and bottom positions of the welded plate. The weld metal region was located at the mid-length position of the transverse test pieces and a gauge length of 50 mm was used in accordance with AS 1391[15].

3. Results and discussion

3.1 Macroscopic and microscopic examination

Macrographs of cross-sections of the welds (Fig. 2) showed no evidence of the common NGW defects of lack of side-wall fusion and slag entrapment[11]. The fusion boundary exhibited a slight undulation because of the shapes of the overlapping weld beads. The width of the weld bead varied from about 12.5 mm to 14 mm for the pulsed welds and was slightly smaller for the non-pulsed welds (12 mm-13.5 mm). These Figs, when compared to the original gap dimensions of 10-12 mm, indicate the extent of side-wall melting. The weld metal was diluted by about 10% to 20% by fusion of the base plate. The slight increase in side-wall fusion for the pulsed welds is consistent with the higher nominal heat input recorded in Table 3. However, the actual heat input should be considered rather than the nominal heat input.

The nominal heat inputs listed in Table 3 are average heat inputs determined from the mean welding voltage V, mean welding current I, and the travel speed S. The average nominal heat input (VI/S) was higher for the pulsed welds (2.88 kJ/mm) than the non-pulsed welds (2.70 kJ/mm), but the actual or effective heat inputs are likely to differ from these values. In particular, the nominal arc efficiency factor, which takes account of heat losses by convection and radiation, is higher for SAW (0.95) compared with GMAW (0.8)[16]. Incorporating these factors modifies the estimates of heat input to 2.57 kJ/mm for non-pulsed SAW and 2.16 kJ/mm for non-pulsed GMAW. These values show a significantly higher heat input for SAW and are likely to be closer to the actual heat inputs. The modified heat inputs for the pulsed welds are 2.74 kJ/mm for SAW and 2.30 kJ/mm

for GMAW. However, these values are less certain because the actual current waveform for the pulsed welds needs to be considered in calculating the thermal energy [17]. Moreover, the features of the welds (Fig. 2) indicate that the heat inputs were lower for the pulsed welds than for the non-pulsed welds. The necessity for an extra weld capping pass for the pulsed SA weld suggests that the weld bead volume was lower than for the non-pulsed weld. Furthermore, the depth of penetration into the backing plate was smaller for both of the pulsed welds, indicating that current pulsing flattens the weld bead and decreases its volume. In addition, the measurements of weld bead widths indicate that side-wall melting is increased for pulsed welding using both SAW and GMAW.

The HAZ is conventionally divided into the following sub-zones or regions: the grain coarsened region (GCHAZ), the grain refined region (GRHAZ) and the intercritical region (ICHAZ). Representative optical micrographs of these regions are given in Fig. 3. The GCHAZ, Fig. 3(a), consisted of fine bainitic ferrite with interlath islands of martensite-austenite constituent (MAC), as well as regions of lath martensite. Electron microscopy was also conducted on foil samples of the GCHAZ of the final weld pass. Fig. 4 shows bainitic ferrite with interlath elongated islands of MAC and a region of lath martensite, distinguished by smaller lath width and the absence of MAC, as shown in Fig. 5. However, lath martensite was less abundant than bainitic ferrite because preheat and interpass heating slowed the cooling rate sufficiently to restrict transformation to martensite, as well as tempering the microstructures that formed. It should be noted that weld beads other than the capping bead are subject to thermal spikes due to deposition of subsequent weld layers. Therefore, substantial and variable tempering is to be expected to occur for sub-surface weld layers.

The GRHAZ, Fig. 3(b), is characterised by refined austenite grains which again transformed to bainitic ferrite, lath martensite, together with some grain boundary particles of ferrite. The ICHAZ, Fig. 3(c) only partially transformed to austenite on heating, followed by transformation on cooling of carbon-enriched austenite to higher carbon products consisting of bainite, nodular pearlite and/or MAC. The untransformed matrix (retained ferrite) consisted of a well-tempered mixture of ferrite and carbide. Although Figs. 3-5 are for NG-SAW, there were essentially no detectable differenceswere found in the HAZ microstructures of the NG-GMA welds.

The overlapping weld beads of the NGW process establish overlapping HAZs and a schematic representation of this feature is shown in Fig. 6. Overlap can be described in terms of 9 overlapping sub-zones of the HAZ[18]. These sub-regions can be described as GC-GC,

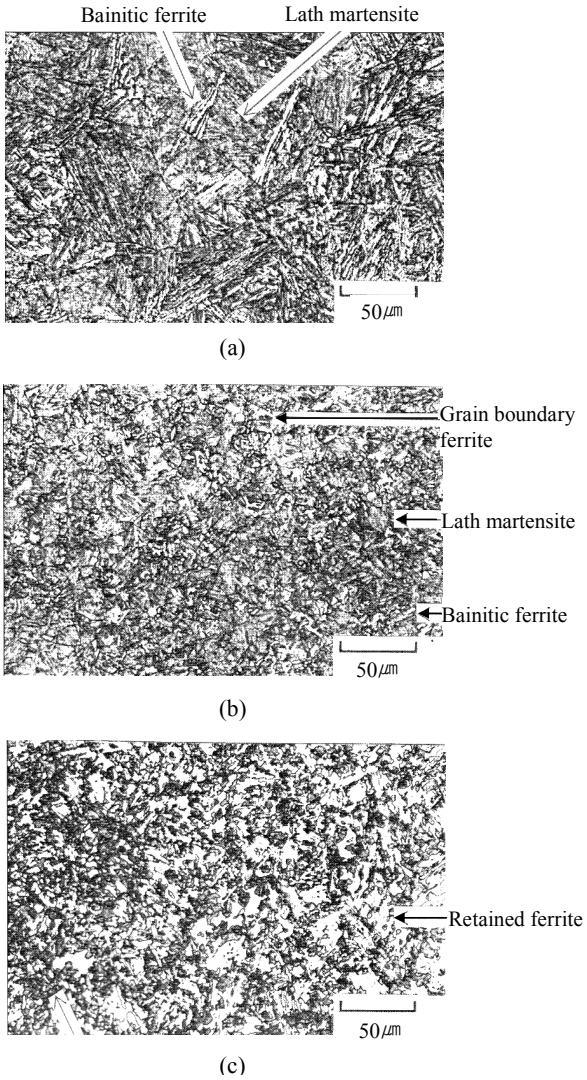

Fig. 3 Optical micrographs of selected regions of the HAZ of the capping pass of a narrow gap weld (SAW): (a) GCHAZ; (b) GRHAZ; and (c) ICHAZ

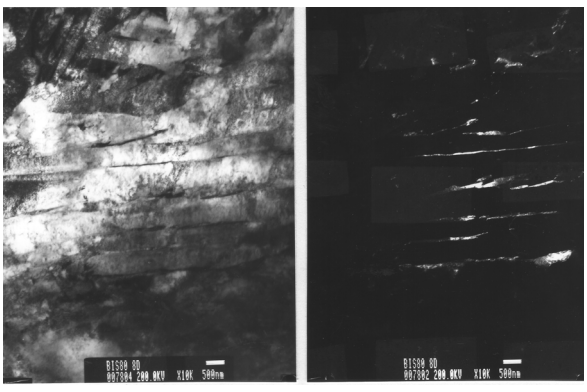

Fig. 4 Transmission electron micrographs showing bainitic ferrite with interlath regions of MAC in GCHAZ of NG-SA weld: (a) bright field; and (b) dark field using austenite diffraction spot

Fig. 5 Transmission electron micrograph showing a region of lath martensite in the GCHAZ of NG-SA weld

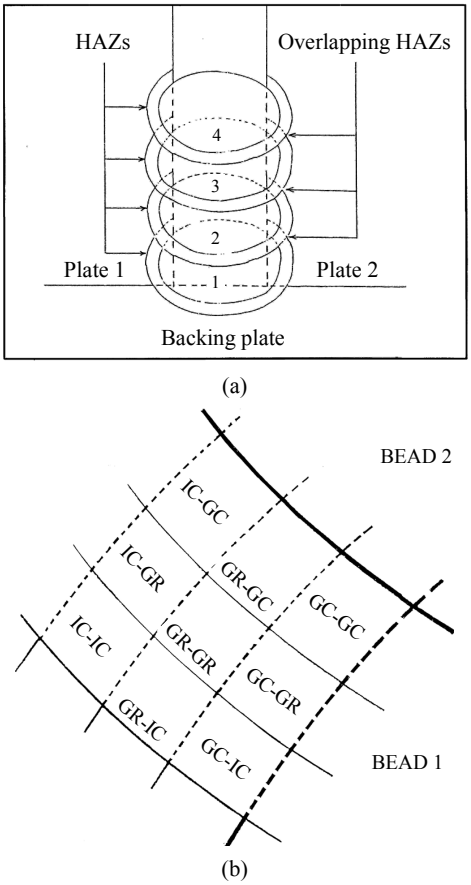

Fig. 6 (a) Schematic diagram showing four one-pass-per-layer welds in a narrow gap between two plates, with a backing plate. The HAZs produced by the welds and the overlapping HAZ regions are identified. (b) Schematic diagram of an overlapping HAZ region produced by depositing weld bead 2 on the previous weld bead (1). The first sub-zone region labelled in each pair represents the effect of bead 1

GC-GR, GC-IC, GR-GC, GR-GR, GR-IC, IC-GC, IC-GR and IC-IC, with the first listed sub-region referring to the effect of weld bead 1 and the second to that of the overlapping weld bead, 2. It has been reported that the GC-IC combination can lead to a local brittle zone (LBZ) because the prior austenite boundaries can be decorated with networks of a brittle product due to the transformation of pools of carbon-enriched grain boundary austenite[19]. An example of this type of sub-region is shown in Fig. 7. The prior austenite grain boundaries are decorated with a network of fine ferrite-carbide aggregate and/or MAC produced by transformation on cooling of austenite formed at these boundaries during reheating. The matrix consists of well- tempered laths of bainite and/or martensite. The concept and significance of the LBZ is discussed later when the Charpy measurements are considered.

Hardness profiles across the HAZ and weld metal were measured 2 mm below the plate surface to test a region that was not thermally affected by a subsequent welding pass. The hardness profiles for the pulsed and non-pulsed GMA welds are shown in the left column of Fig. 8 and those for the SA welds are presented in the right column.

Fig. 8 shows that the average weld metal and base plate hardness values were closely similar (~ 300 HV10), but there was pronounced softening of the parent plate adjacent to the observed boundary of the HAZ. This effect, which is due to tempering of the Q&T steel in the subcritical zone, appeared to be slightly more pronounced for the GMA welds. Although Fig. 8 also indicates that the HAZ width was higher for the pulsed welds (4.9 – 5.0 mm) than those for the non-pulsed welds (about 4.8 mm), these measurements relate to the capping passes which show atypical HAZ widths, see Fig. 2. Moreover, the pulsed SA weld required two capping passes, changing the contour of the HAZ. The average HAZ width was about 3 mm for all welds.

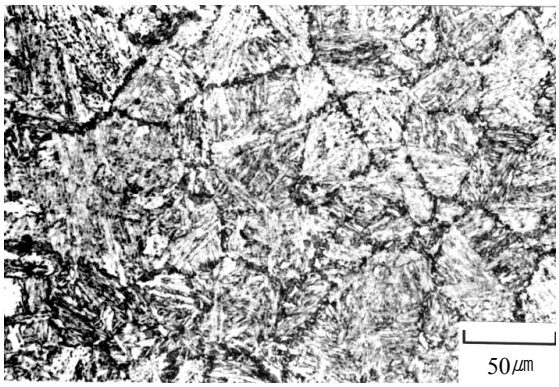

Fig. 7 GC-IC sub-region of the HAZ of the pulsed SA narrow gap weld. Nominal heat input of 2.88 kJ/mm

The peak HAZ hardness for the non-pulsed welds was higher (440 HV10) for GMAW than for SAW (420 HV10). The hardness difference was similar for the pulsed welds. These observations are consistent with the heat inputs calculated by incorporation of the arc efficiency. These heat inputs are 2.57 kJ/mm for non-pulsed SAW and 2.16 kJ/mm for non-pulsed GMAW. The corresponding heat inputs for pulsed welding are 2.74 and 2.30 kJ/mm, but these values are likely to be over-estimates because no consideration was taken of the effect of current pulsing. A higher heat input reduces the cooling rate in the HAZ region of the weld allowing the transformation of austenite to softer ferritic products.

It should also be noted that the maximum HAZ hardness for all of the hardness profiles shown in Fig. 8 is skewed away from the GCHAZ towards the GRHAZ. This phenomenon has been reported previously by the authors for welded Q&T steels and is referred to as the displaced hardness peak effect[20,21].

Although hardness profiles were not measured at different depths below the surface, it is to be expected that the peak hardness will drop progressively with depth because of cumulative re-tempering due to the thermal impact of subsequent weld passes.

3.2 Tensile testing

Transverse tensile tests were conducted on samples taken from the top (T), centre (C) and bottom (B) regions of the NG welds, Table 4. All fractures occurred in the weld metal and had a cup-and-cone appearance. These results show that the weld metal strength decreased and the ductility increased from the top to the bottom of the weld due to the progressive variation of the extent of in-process tempering associated with gap filling.

The tensile strength values exceeded those of the base plate (805 MPa), but %ROA values were slightly lower and the %elongation was substantially lower than the 26% recorded for the base plate. This latter result probably arises from the strength and rigidity of the HAZ layers lying within the gauge length, together with the presence of non-metallic inclusions in the weld metal which facilitate void formation and coalescence, thus resulting in more limited plastic deformation before failure with cup-and-cone fracture appearance. Although the values of hardness and the tensile strength indicate that the weld metal and base plate are closely matched in tensile properties, fracture occurred in the weld metal. This failure site is likely to be associated with the

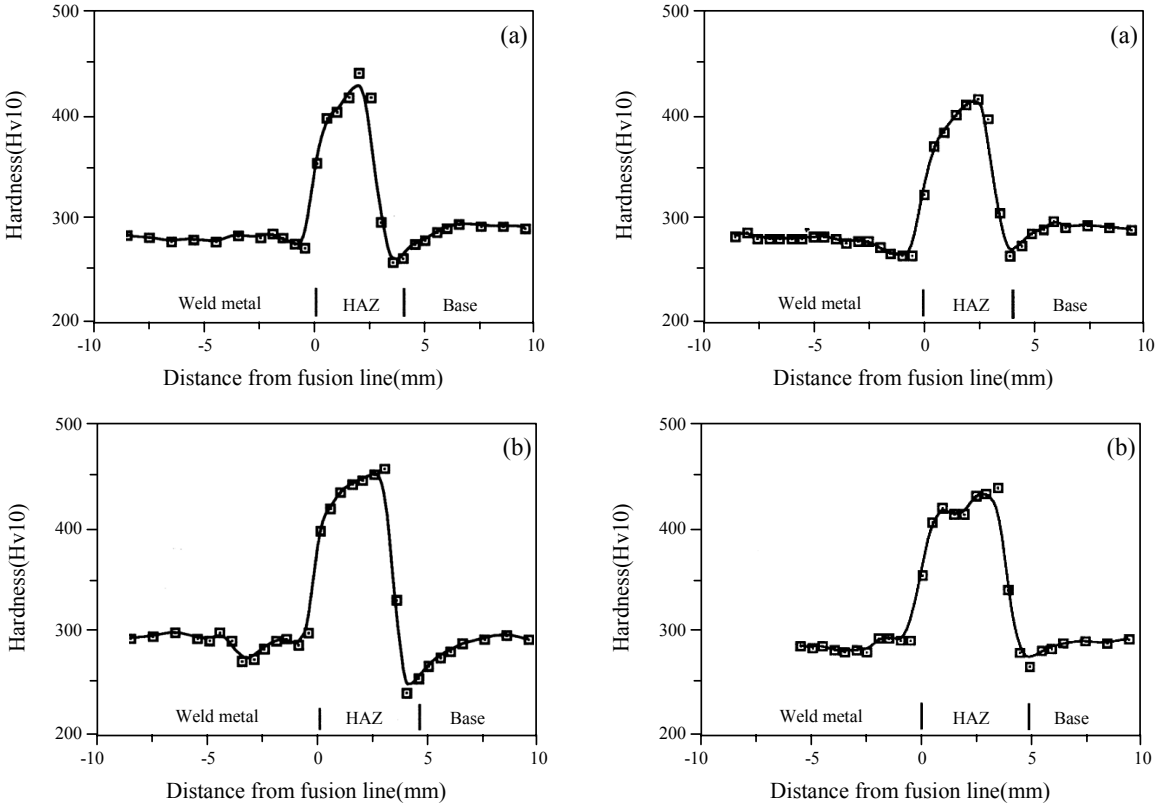

Fig. 8 Hardness profiles across weld cross-sections of NG welds, 2 mm below the plate surface, for GMAW (left column) and SAW (right column). The symbol "a" in the right top corner of graphs identifies the non-pulsed welds and "b", the pulsed welds

Table 4 Tensile properties of cross-weld samples taken from the top (T), centre (C) and bottom (B) regions of the narrow gap welds

Sample	Position	UTS (MPa)	% ROA	% ELONG. (50 mm GL)	Fracture Location
Pulsed SAW	T	844	62	12	Weld
	C	820	68	13	Weld
	B	794	72	13	Weld
Non-pulsed SAW	T	834	64	10	Weld
	C	815	66	11	Weld
	B	798	70	12	Weld
Pulsed GMAW	T	841	63	11	Weld
	C	819	69	11	Weld
	B	799	70	12	Weld
Non-pulsed GMAW	T	836	65	10	Weld
	C	817	67	12	Weld
	B	801	68	12	Weld

presence of abundant non-metallic inclusions that provide nucleation sites for void formation.

Charpy impact testing

CVN tests at -20℃ for the weld metal and the HAZ were highly variable, ranging from 20 to150 J (Table 5). Mean values based on four measurements were in the range 109 to 86 J for weld metal and in the range 100 to 35 J for HAZ samples. General trends were that (1) weld metal CVN values were higher than those for the HAZ and had lower standard deviations; and (2) the SAW weldments showed higher CVN values, particularly for the HAZ samples. The lower CVN values for the GMA weld metals is likely to arise from a higher concentration of oxide inclusions due to the relatively high oxidising potential of 11.5% for the shielding gas ($OP\% = O_2+1/2\ CO_2$). Variability of the HAZ Charpy results is to be expected because of uncertainty in the location of the notch within the narrow HAZ (about 3 mm wide). The notch root can be located in regions with variable amounts of GC, GR and IC zones, as well as in the overlapping HAZ sub-regions indicated in Fig. 6(b). It should be noted, however, that the volume fraction of the local brittle zone (GC-IC) sub-region (see Fig. 7) is relatively small and would be unlikely to exert a controlling influence on fracture resistance. Although variable HAZ microstructures will apply to Charpy tests for both SA and GMA welds, the results for the SA welds were significantly higher. As discussed below, the differences in HAZ Charpy values are likely to be associated with variations in effective heat input and heat transfer paths and the resulting influence on the thermal profile experienced by the HAZ.

The high oxygen potential of the GMAW shielding gas is expected to increase the temperature of the molten weld metal and promote the formation of a more penetrating weld bead with a relatively large fusion zone. However, heat loss from the surface of the solidifying weld bead by convection and conduction into the base plate is expected to be more rapid for the GMA welds, since the SA weld is insulated by the flux layer until it is removed after completion of the weld layer. These factors are taken into account by the arc efficiency which, despite the effect of active gas shielding, is significantly lower for GMAW (0.8) than for SAW (0.95). The heat inputs calculated by incorporation of the arc efficiency are 2.57 kJ/mm for non--pulsed SAW and 2.16 kJ/mm for non-pulsed GMAW. The corresponding values for pulsed welding are 2.74 and 2.30 kJ/mm. The higher heat inputs for NG-SAW reduce the cooling rate in the HAZ region of the weld allowing the transformation of austenite to ferritic products over a higher temperature range, leading to a lower dislocation density and more sustained autotempering (formation and coarsening of carbide precipitates). The lower HAZ peak hardness values observed for the NG-SA welds are consistent with this interpretation. The higher Charpy values observed for the HAZ of the SAW welds can also be rationalised in this way.

4. Conclusions

Successful NG welds were obtained in 50 mm thick Q&T steel plate using a one-pass-per-layer technique for both the GMAW and SAW processes. Pulsing of the welding current had the effect of slightly increasing side-wall fusion, flattening the weld bead and decreasing its volume.

The tensile strength and impact energy of the weld

metal exceeded those of the base plate for all welds. However, the tensile ductility of cross-weld samples was substantially lower and the maximum HAZ hardness exceeded that of the base steel by more than 100 HV points.

Although Charpy values for the HAZ were variable because of variations in the microstructures of regions underlying the notch, they were higher for the SAW welds. Further, the peak HAZ hardness was about 20 HV points lower for these welds.

These differences arise because different thermal cycles are associated with the two welding processes. Although the average nominal heat inputs were the same, the effective heat inputs differed because of the different shielding methods and weld bead profiles. Incorporating arc efficiency factors resulted in estimates of heat inputs of 2.57 kJ/mm for non-pulsed NG-SAW and 2.16 kJ/mm for non-pulsed NG-GMAW. The corresponding values for pulsed welding (2.74 and 2.30 kJ/mm) are likely to be over-estimates because the effect of current pulsing was not taken into account. Nevertheless, the effective heat input was higher for NG-SAW, with the consequence of a lower cooling rate in the HAZ region of the weld which promotes the transformation of austenite at higher temperatures to softer ferritic products. The lower HAZ peak hardness and the higher HAZ Charpy values for SAW are consistent with lower weld cooling rates than those for the GMA welds.

Acknowledgements

The authors would like to acknowledge the significant inputs of Dr-Ing. Nasir Ahmed and other members of the welding research laboratory of CSIRO, Adelaide, South Australia. Comments on the manuscript by Emeritus Professor John Norrish of the University of Wollongong, NSW, Australia, are also acknowledged with gratitude.

ORCID: Druce Patrick Dunne: http://orcid.org/0000-0002-9115-320X
ORCID: Willy Pang: http://orcid.org/0000-0003-2641-1310

References

1. R.P. Meister and D.C. Martin, *British Welding Journal*, 13 (5) (1966), 252
2. Y. Sejima, T. Godai, M. Kawahara and H. Nomura, IIW XII-A-006-81 and IIW XII-B-10-81, *Applications of Narrow Gap Welding Process in Japan*
3. V. Malin, The state of the art of narrow gap welding part 1, *Welding Journal*, 62(6) (1983), 22
4. V. Malin, Monograph on Narrow Gap Welding Technology, *WRC Bulletin 323*, Welding Research Council, New York, (1987)
5. Chen Zhang, Geng Li, Ming Gao, Xiao Yan Zang, Microstructure and mechanical properties laser-arc hybrid welded 40 mm thick mild steel, *Materials*, 10 (2017), 106
6. J. Wang, J. Zhu, P. Fu, R, Su, W. Han and F. Yang, A swinging arc system system for narrow gap GMA welding, *ISIJ*, 52 (2012), 110-114
7. J.Y. Wang, Y,S. Ren, F. Yang, H.B. Guo, Novel rotation arc system for narrow gap MAG welding, *Sci. and Tech. of Welding and Joining*, 12 (2007), 505-507
8. T. Ohnishi, Y. Kawahito, M. Mizutani, and S. Katayama, Butt welding of thick high strength steel plate with a high power laser and hot wire to improve tolerance to gap variation and control weld metal oxygen, *Sci. and Tech. of Welding and Joining*, 18 (2013), 314-322
9. TWI Technical Note, What is narrow gap welding?, www.twi-global.com/technical
10. I.D. Henderson, Narrow gap welding - a process for joining HSLA steels, in High Strength Low Alloys Steels, *Proceedings of Int. Conf. on HSLA Steels*, ed. by D.P. Dunne and T. Chandra, Wollongong, NSW, Australia, 124-128, (1984)
11. W. Pang, The Structure and Properties of the Heat Affected Zone of Structural Plate Steels Welded by High Productivity rocesses, *PhD Thesis, University of Wollongong*, NSW, Australia, (1993)
12. Australian Standard, AS 2205.6.1, Methods of Destructive Testing of Welds in Metal, Part 6.1, Hardness Test, Weld Joint Hardness Test, *Standards Australia*, (1989)
13. Australian Standard, AS 1544.2, Methods for Impact Tests on Metals,Part 2, Charpy V-Notch, *Standards Australia*, (1989)
14. Australian Standard, AS 2205.7.1, Methods for Destructive Testing of Welds in Metals, Part 2.1, Toughness Test-Charpy V-Notch Impact Test, *Standards Australia*, (1980)
15. Australian Standard, AS 1391, Methods for Tensile Testing of Materials, *Standards Australia*, (1991)
16. O. Grong, Metallurgical Modelling of Welding, I*nstitute of Materials*, London, (1994)
17. J. Norrish, IIW-Doc-XII-2306-16, Recent Gas Metal Arc Welding (GMAW) Process Developments, The implications related to International fabrication standards, *Welding in the World*, (2017)
18. Druce Dunne, Huijun Li and Christopher Jones, Re-austenisation of chromium-bearing pressure vessel steels during the weld thermal cycle, *Australasian Welding Journal, Weld. Res. Supplement*, 56(2) (2013), 36-48
19. D.P. Fairchild, Local brittle zones in structural welds, in Welding Metallurgy of Structural Steels, (1987), ed. by J.Y. Koo, TMS-AIME, Warrendale, PA, *USA*, 303-318
20. W. Pang, N. Ahmed and D. Dunne, Hardness and mi-

crostructural gradients in the heat affected zone of welded low-carbon quenched and tempered steels, *Australasian Welding Journal, Weld. Res. Supplement*, 58(1) (2011), 39-48

21. D.P. Dunne and W. Pang, Displaced hardness peak phenomenon in heat-affected zone of welded quenched and tempered EM812 steel, *Welding in the World*, 61(1) (2017), 57-67